Atmos. Meas. Tech. Discuss., 4, 1255–1302, 2011
www.atmos-meas-tech-discuss.net/4/1255/2011/
doi:10.5194/amtd-4-1255-2011

Atmospheric Measurement Techniques Discussions

Detection of HO_2 by laser-induced fluorescence: calibration and interferences from RO_2 radicals

H. Fuchs, B. Bohn, A. Hofzumahaus, F. Holland, K. D. Lu, S. Nehr, F. Rohrer, and A. Wahner

Institute of Energy and Climate Research: Troposphere (IEK-8), Forschungszentrum Jülich GmbH, Jülich, Germany

Received: 9 February 2011 – Accepted: 18 February 2011 – Published: 25 February 2011

Correspondence to: H. Fuchs (h.fuchs@fz-juelich.de)

Published by Copernicus Publications on behalf of the European Geosciences Union.

Abstract

HO_2 concentration measurements are widely accomplished by chemical conversion of HO_2 to OH including reaction with NO and subsequent detection of OH by laser-induced fluorescence. RO_2 radicals can be converted to OH via a similar radical reaction sequence including reaction with NO, so that they are potential interferences for HO_2 measurements. Here, the conversion efficiency of various RO_2 species to HO_2 is investigated. Experiments were conducted with a radical source that produces OH and HO_2 by water photolysis at 185 nm, which is frequently used for calibration of LIF instruments. The ratio of HO_2 and the sum of OH and HO_2 concentrations provided by the radical source was investigated and was found to be 0.50 ± 0.02. RO_2 radicals are produced by the reaction of various organic compounds with OH in the radical source. Interferences via chemical conversion from RO_2 radicals produced by the reaction of OH with alkanes (H-atom abstraction) are negligible consistent with measurements in the past. However, RO_2 radicals from OH plus alkene- and aromatic-precursors including isoprene (mainly OH-addition) are detected with a relative sensitivity larger than 80% with respect to that for HO_2 for the configuration of the instrument with which it was operated during field campaigns. Also RO_2 from OH plus methyl vinyl ketone and methacrolein exhibit a relative detection sensitivity of 60%. Thus, previous measurements of HO_2 radical concentrations with this instrument were biased in the presence of high RO_2 radical concentrations from isoprene, alkenes or aromatics, but were not affected by interferences in clean air, when the OH reactivity was dominated by small alkanes. By reducing the NO concentration and/or the transport time between NO addition and OH detection, interference from these RO_2 species are suppressed to values below 20% relative to the HO_2 detection sensitivity. The HO_2 conversion efficiency is also smaller by a factor of four, but this is still sufficient for atmospheric HO_2 concentration measurements for a wide range of conditions.

AMTD
4, 1255–1302, 2011

1 Introduction

The measurement of hydroperoxy radical (HO_2) concentrations is important for the understanding of the photochemical degradation of atmospheric trace gases and the formation of secondary air pollutants such as ozone (e.g., Finlayson-Pitts and Pitts Jr., 2000). HO_2 is mainly produced by radical chain reactions, starting with the reaction of CO or volatile organic compounds (VOC) with photochemically produced hydroxyl radicals (OH). It is also formed by the photolysis of carbonyl compounds, ozonolysis and the reaction of the nitrate radical (NO_3) with organic compounds (e.g., Geyer et al., 2003; Kanaya et al., 2007).

Because of the small radical concentrations in the atmosphere within the range of some ten parts per trillion per volume (pptv) (e.g. Monks, 2005; Kanaya et al., 2007; Lelieveld et al., 2008; Hofzumahaus et al., 2009) high instrument sensitivities are required for the detection of HO_2. Matrix Isolation Electron Spin Resonance Spectroscopy (MIESR) is the only known technique being capable of specific HO_2 measurements in the atmosphere, but requires relatively long integration times (30 min) (Mihelcic et al., 1985, 1990).

Laser induced fluorescence (LIF) allows a more sensitive HO_2 detection, at integration times of about 1 min. It applies chemical conversion of HO_2 to OH at reduced pressure and detects OH by LIF (see review, Heard and Pilling, 2003). Chemical conversion combined with radical amplification is used by Peroxy Radical Chemical Amplifier (PERCA) (Cantrell et al., 1984; Hastie et al., 1991; Clemitshaw et al., 1997; Burkert et al., 2001; Sadanaga et al., 2004; Mihele and Hastie, 2000; Green et al., 2006; Andrés-Hernández et al., 2010) and Peroxy Radical Chemical-Ionization Mass Spectrometry (ROxMas, PerCIMS) (Hanke et al., 2002; Edwards et al., 2003; Hornbrook et al., 2011), in order to achieve high measurement sensitivities for HO_2. All indirect techniques (LIF, PERCA and ROxMas/PerCIMS) make use of the conversion reaction between HO_2 and NO, in order to produce OH. Possible loss of OH by formation of

AMTD
4, 1255–1302, 2011

nitrous acid (HONO) can be suppressed by lowering the pressure in the measurement systems.

$$HO_2 + NO \rightarrow OH + NO_2 \quad \text{(R1)}$$

$$OH + NO + M \rightarrow HONO + M \quad \text{(R2)}$$

M is any collision partner, mostly oxygen and nitrogen.

Organic peroxy radicals (RO_2) are present in the atmosphere at similar concentrations as HO_2. RO_2 is mainly produced in the reactions of OH, O_3 and NO_3 with organic compounds. Reactions of VOCs with OH take place either via H-atom abstraction or addition of OH leading to two different types of RO_2 radicals (Atkinson and Arey, 2003). RO_2 radicals react with NO at nearly the same rate as HO_2.

$$RO_2 + NO \rightarrow RO + NO_2 \quad \text{(R3)}$$

$$RO + O_2 \rightarrow R'CHO + HO_2 \quad \text{(R4)}$$

$$RO + NO \rightarrow RONO \quad \text{(R5)}$$

In HO_2 detection systems that apply chemical conversion HO_2 produced by Reaction (R4) can undergo further conversion to OH (Reaction R1). This is utilized by PERCA and ROxMas/PerCIMS instruments, and one specialized LIF instrument, ROx-LIF (Fuchs et al., 2008), in order to measure the sum of HO_2 and RO_2 (= RO_x). PERCA instruments cannot distinguish between HO_2 and RO_2. ROxMas/PerCIMS instruments, however, modulate the chemical conditions in their instruments, in order to measure either RO_x, or HO_2 only. The HO_2 measurement mode requires good suppression of the RO_2 to HO_2 conversion. Edwards et al. (2003), for example, achieved a suppression to less than 15% in their PerCIMS instrument for RO_2 species that were produced by the reaction of Cl with various hydrocarbons. However, this required large changes in concentrations of reactants, so that the modulation between HO_2 and RO_x measurement mode took 30 min. In order to achieve a faster switching of the measurement modes

AMTD
4, 1255–1302, 2011

within 1 min, Hornbrook et al. (2011) lowered the reactant concentrations in the HO_2-mode. The new method that improves temporal resolution offers good discrimination between HO_2 and various alkyl peroxy radicals, but RO_2 from the reaction of OH with large alkanes, alkenes (including isoprene) and aromatics are partially or fully detected in the HO_2-mode of this instrument. RO_2 radicals were produced by the reaction of OH in Hornbrook et al. (2011), so that radical species from the same organic precursor were not necessarily the same as in Edwards et al. (2003).

It is generally believed that RO_2 radical conversion via Reactions (R3), (R4) and (R1) in the detection cell of LIF instruments for HO_2 measurements is negligible (Heard and Pilling, 2003). Experimental investigations in the laboratory for C_1–C_4 alkyl peroxy radicals and results from field campaigns (Stevens et al., 1994; Mather et al., 1997; Kanaya et al., 2001; Creasey et al., 2002; Ren et al., 2004; Fuchs et al., 2010) did not hint towards a significant interference. For example, for the instrument characterized here, it was shown that the upper limit for an interference from methyl peroxy radicals (CH_3O_2) is 5% (Weber, 1998; Holland et al., 2003). The reason for the suppression of OH formation from CH_3O_2 radicals is the slow rate of Reaction (R4) at the low-pressure condition in the instrument. Only a small fraction of CH_3O is eventually converted to OH within the reaction time of a few milliseconds between the injection of NO and detection by the laser beam. Moreover, Reaction (R4) competes with the formation of nitrite in the presence of high NO concentrations (Reaction R5). However, the potential for an interference from organic peroxy radicals from alkenes, aromatics and OVOCs was not experimentally studied assuming that these RO_2 radicals would behave like small alkyl peroxy radicals.

So far, only few intercomparisons of HO_2 concentration measurements from different instruments have been performed at atmospheric conditions. The HO_2 comparisons in ambient air between LIF and MIESR (Platt et al., 2002) and between LIF and PerCIMS (Ren et al., 2003) exhibited high correlations and good absolute agreement without hints towards significant interferences. Recently, however, Ren et al. (2008) reported a change of the calibration factor of the LIF instrument. This may possibly require

AMTD
4, 1255–1302, 2011

revision of the comparison results. Good agreement was also found for measurements from ROxLIF and MIESR in chamber measurements, during which HO_2, CH_3O_2 and $C_2H_5O_2$ were specifically measured (Fuchs et al., 2009). However, unexplained differences were observed between three LIF instruments in the international comparison campaign HOxComp (Fuchs et al., 2010), when measurements were taken in ambient air and in chamber experiments. Although the data from different instruments were well-correlated, the linear regressions showed sometimes differences that exceeded the combined estimated measurement errors and exhibited an unexplained water vapor dependence. The results from this campaign point to potential interferences in the calibration or measurement techniques.

Therefore, we investigated (1) the yield of radicals in the calibration source that produces OH and HO_2 radicals by water photolysis at 185 nm and (2) the potential for an interference from various RO_2 radical species in HO_2 concentration measurements. RO_2 radicals are produced by the reaction of organic compounds with OH in the calibration source. An interference from RO_2 radicals would impact HO_2 concentration measurements in the past, when high loads of VOCs including isoprene were present such as during the field campaigns ECHO (Kleffmann et al., 2005; Dlugi et al., 2010) and PRIDE-PRD2006 (Hofzumahaus et al., 2009; Lu et al., 2011).

2 Detection of HO_2 radicals

HO_2 radicals cannot be detected directly by LIF. However, they can be chemically converted to OH, so that the detected OH concentration represents the sum of HO_2 and OH ($= HO_x$) in the sampled air (Hard et al., 1984; Heard and Pilling, 2003). A description of our LIF instrument has been given by Holland et al. (2003). The main instrument parameters are summarized in Table 1 and a schematic drawing of the detection cell is given in Fig. 1. The instrument performed measurements in two configurations: In the first configuration, 0.28 slpm (liter per minute at 1 atm and 20 °C) of air is drawn into a detection cell at low pressure of 3.5 hPa through a conically shaped inlet nozzle

AMTD
4, 1255–1302, 2011

(Beam Dynamics) with an orifice of 0.2 mm. Configuration 2 differs in the orifice size of the inlet nozzle (0.4 mm), so that 1.1 slpm is drawn into the detection cell. The latter instrument configuration was used in past field campaigns and for experiments in the simulation chamber SAPHIR in Jülich.

The air stream in the detection cell is crossed by a short laser pulse at 308 nm (25 ns duration, 8 mm diameter, 8.5 kHz repetition rate, 25 mW average power at 308 nm), which is provided by a Nd:YAG pumped dye laser system (Navigator Spectraphysics and Intradye Laser Analytical Systems), approximately 10 cm downstream of the tip of the inlet nozzle (Fig. 1). OH is excited on a single rovibronic transition ($Q_{11}(3)$ line of the $A^2\Sigma - X^2\Pi(0,0)$ transition). The resonance fluorescence is measured by gated photon counting using a time delay, in order to discriminate the OH fluorescence from the instantaneous laser stray light.

Chemical conversion of HO_2 to OH is accomplished by its reaction with NO (Reaction R1). Different flows of NO were injected into the sampled gas. During the ECHO and HOxComp campaigns, 4 sccm (1 sccm = 1 cm^3/min at 298 K and 1 atm) of pure NO were added through a ring made of glass tubing with small holes, surrounding the gas expansion. During the PRIDE-PRD2006 campaign, 1 sccm of NO was injected by a glass tube with a small orifice that reached into the gas expansion. The concentration of NO was chosen that the HO_2 conversion efficiency is larger than 90% within the travel time of the sampled gas between NO addition and laser excitation (distance here: 5.5 cm). No significant difference was found in this work between using the glass ring or glass tube for NO addition. The NO was always purified in a cartridge that was filled with Ascarite (sodium hydroxide-coated silica) prior to addition, in order to minimize artificial signals from impurities.

AMTD
4, 1255–1302, 2011

3 Calibration of the detection sensitivity

3.1 The radical source

In order to calibrate the sensitivity of the LIF instrument, a radical source provides accurately known radical concentrations. This is accomplished by the photolysis of water in air at 1 atm using 185 nm radiation of a low-pressure discharge mercury lamp (Aschmutat et al., 1994; Schultz et al., 1995; Heard and Pilling, 2003):

$$H_2O + h\nu \rightarrow OH + H \qquad (\lambda = 184.9\,\text{nm}) \tag{R6}$$

Characterization measurements reported here are done with the calibration source described in detail by (Holland et al., 2003). Typical radical concentrations are $7 \times 10^9\,\text{cm}^{-3}$, but can be lowered by a factor of 100 by reducing the intensity of the radiation, when the light passes an absorption cuvette filled with N_2O (not done here). Humidified synthetic air of highest purity (99.9999%) flows through a 60 cm long glass tube (inner diameter 1.9 cm) at a high flow rate of $20\,\text{l}\,\text{min}^{-1}$ (laminar flow). The radiation of a mercury lamp crosses the air approximately 6 cm upstream of the inlet nozzle of the instrument, which sticks into the glass tube. The transport time of the radicals produced by photolysis (Reaction R6) is approximately 20 ms, before the gas flow reaches the tip of the inlet nozzle. The absolute radical concentration provided by the calibration source can be related to the amount of ozone that is simultaneously formed by the photolysis of oxygen at 185 nm in the air flow (Aschmutat et al., 1994; Schultz et al., 1995):

$$O_2 + h\nu \rightarrow O + O \tag{R7}$$

$$O + O_2 + M \rightarrow O_3 + M \tag{R8}$$

Here, this is accomplished indirectly by observing the light intensity measured by a CS–I-phototube, which was calibrated against ozone production. Spectral characteristics of the phototube and an interference filter (185 nm, FWHM = 27.5 nm) in front of

AMTD
4, 1255–1302, 2011

the phototube ensure that only radiation which is relevant for the photolysis is detected by the phototube. The concentration of OH radicals produced by the calibration source can be calculated as:

$$[OH]_0 = [O_3] \frac{\Phi_{OH}[H_2O]\sigma_{H_2O}}{\Phi_{O_3}[O_2]\sigma_{O_2}} \quad (1)$$

Φ_{OH} and Φ_{O_3} are the quantum yields for OH and O_3. The absorption spectrum of oxygen is highly structured in the Schumann-Runge bands around 185 nm. Therefore, the value of the absorption cross section, σ_{O_2}, is specific for every mercury lamp and depends on the special design of the radical source (Hofzumahaus et al., 1996; Cantrell et al., 1997). The absorption cross section of water, σ_{H_2O}, does not show distinctive structures and is well-known (Hofzumahaus et al., 1996; Cantrell et al., 1997; Creasey et al., 2003). The quantum yield of ozone in 1 atm of air is assumed to be $\Phi_{O_3} = 2$, supported by the experimental study by Washida et al. (1971). For OH, the quantum yield is generally assumed to be one based on spectroscopic considerations.

3.2 OH and HO_2 yields in the radical source

Photolysis of water molecules at 185 nm has only one energetically and spin-allowed dissociation channel, leading to $OH(^2\Pi) + H(^2S)$ with both fragments in their electronic ground states (Reaction R6). The photo-dissociation process occurs in the first absorption band of water and is experimentally and theoretically one of the best understood polyatomic photo-dissociation processes (Engel et al., 1992). Upon photon absorption, the excited H_2O molecule decomposes rapidly in less than an internal vibrational period. Unity quantum yield is therefore expected for OH from Reaction (R6). OH radicals are produced almost exclusively in their vibrational ground state and most of the excess energy (≈ 1.58 eV) from the photo-dissociation is transferred into translation of the H-atoms. The highly energetic H-atoms can undergo several chemical reactions or loose their energy by collisions with other molecules:

$$H^* + H_2O \rightarrow OH + H_2 \quad (R9)$$

AMTD
4, 1255–1302, 2011

$$H^* + O_2 \rightarrow OH + O \quad \text{(R10)}$$

$$H^* + M \rightarrow H + M \quad \text{(R11)}$$

$$H + O_2 + M \rightarrow HO_2 + M \quad \text{(R12)}$$

Because Reaction (R11) quickly removes excess energy, it is generally assumed that the H-atoms from water photolysis are completely converted to HO_2 (Reaction R12). However, Reactions (R9) and (R10) are energetically possible, if the H-atoms carry translational energy greater than 0.7 eV (Bajeh et al., 2001; Zhang et al., 2000), which is the case at 185 nm. In order to investigate the relevance of OH formation from Reactions (R9) and (R10), the HO_x partitioning in the calibration gas is measured, when humidified synthetic air is irradiated by 185 nm at 1 atm, room temperature and 30% relative humidity. The experiment is performed in two steps. First, an amount of 60 ppmv CO is added as an OH scavenger, in order to convert all OH to HO_2 within the residence time ($\approx$ 20 ms) between photolytical generation and intake into the detection cell.

$$OH + CO + O_2 \rightarrow HO_2 + CO_2 \quad \text{(R13)}$$

In this mode, the sum of OH and HO_2 is measured. OH that is produced by water photolysis (Reaction R6) and Reactions (R9) and (R10) is converted to HO_2 and is measured in the detection cell together with HO_2 produced by Reactions (R11) and (R12). Overall, this calibration mode has an HO_2 yield of 2 independent of Reactions (R9) and (R10). Second, 0.1% deuterated methane (CD_4) is used as an scavenger, which ultimately removes OH in the calibration gas.

$$OH + CD_4 + O_2 \rightarrow CD_3O_2 + HDO \quad \text{(R14)}$$

In this mode, HO_2 is formed by Reactions (R11) and (R12), only. If the competing Reactions (R9) and (R10) play a role, H atoms are converted to OH and the yield of HO_2

AMTD
4, 1255–1302, 2011

from Reaction (R12) is diminished, accordingly. Products of the OH-scavenging Reaction (R14) will not interfere, because the deuterated CD_3O_2 radicals cannot be converted to hydrogen-containing HO_x radicals, which would be detectable at the probing laser wavelength. Overall, the calibration mode with CD_4 has an expected HO_2 yield of one, if Reactions (R9) and (R10) are negligible, or less less than one, if H-atoms are removed by Reactions (R9) or (R10).

Figure 2 shows an example of signals from one experiment, when either CO or CD_4 is added to the humidified air in the calibration source. The ratio of the signals gives the ratio of HO_2 to HO_x radicals produced in the radical source. The experiment was repeated four times on different days. The mean of the ratio is 0.50 ± 0.02, meaning a ratio of quantum yields for OH and HO_2 of one in the photolysis of water in air. This result proofs that the assumption of equal OH and HO_2 production in the photolysis of water at 185 nm is justified.

3.3 HO_2 and RO_2 yields of the radical source

The radical source can be operated to provide only HO_2 radicals by adding 60 ppmv CO to the synthetic air, in order to convert OH to HO_2 quantitatively (Reaction R13). This way the source provides HO_2 radicals with a quantum yield of two (HO_2-mode) in contrast to a yield of one without the addition of an OH scavenger (HO_x-mode). Therefore, the HO_2 concentration in the HO_2-mode is twice as large as the OH concentration defined in Eq. (1).

In a similar way, specific RO_2 radicals can be generated by scavenging all OH radicals with a hydrocarbon (Fuchs et al., 2008; Qi et al., 2006; Hornbrook et al., 2011). This is called the RO_x-mode mode of the calibration source. Again, the concentration of organic compounds is chosen, so that all OH is consumed within the time between production of OH in the radical source and sampling by the instrument (OH reactivity approximately $300\,s^{-1}$). Different types of reactions can occur: (1) RO_2 radicals can be produced via H abstraction in the case of alkanes leading to alkyl peroxy radicals. (2) For other organic compounds like alkenes OH addition leads to the formation of

AMTD
4, 1255–1302, 2011

β-hydroxyalkyl peroxy radicals (Atkinson and Arey, 2003). If RO_2 radicals are the only radical product, the source yields equal concentrations of RO_2 and HO_2. However, the yield of RO_2 radicals can differ from unity, if other product channels compete with RO_2 formation in the reaction of OH and the hydrocarbon. For example, it is known that part of the products of benzene with OH is HO_2 (prompt HO_2) and only 35% is RO_2 (Nehr et al., 2011).

3.4 Calibration of detection sensitivities

For calibration of OH, HO_2 and RO_2 sensitivities, C_i, the radical source is operated either in the HO_x-, HO_2- or RO_x-mode. Sensitivities defined here and throughout this report always refer to sensitivities of the HO_2-cell, when NO is added into the detection cell. The fluorescence signal measured by the LIF instrument in the three operational modes of the radical source are:

$$S_{HO_x} = C_{HO_2}\phi_{HO_2}[OH]_0 + C_{OH}\phi_{OH}[OH]_0 = \left(C_{HO_2} + C_{OH}\right)[OH]_0 \quad (2)$$

$$S_{HO_2} = C_{HO_2}\phi'_{HO_2}[OH]_0 = 2C_{HO_2}[OH]_0 \quad (3)$$

$$S_{RO_x} = C_{HO_2}\phi''_{HO_2}[OH]_0 + C_{RO_2}\phi_{RO_2}[OH]_0 = \left(C_{HO_2}(1+\delta) + C_{RO_2}(1-\delta)\right)[OH]_0 \quad (4)$$

ϕ_{HO_2}, ϕ'_{HO_2} and ϕ''_{HO_2} are the HO_2 yields in the three modes of the radical source and ϕ_{OH} and ϕ_{RO_2} the yields of OH and RO_2 in the HO_x- and RO_x-mode, respectively, as discussed in the previous section. The concentration $[OH]_0$ is calculated from Eq. (1). δ is the yield of prompt HO_2 in the reaction of organic compounds with OH without the formation of RO_2 on the time scale of the transport time in the radical source (20 ms).

In order to calculate the HO_2 detection sensitivity, only one measurement with the radical source in the HO_2-mode is required. In contrast, the OH sensitivity of the HO_2 detection cell can be calculated from the difference between measurements with the radical source in the HO_2- and HO_x-mode and the RO_2 sensitivity from the difference between measurements in the HO_2- and RO_x-mode:

AMTD
4, 1255–1302, 2011

$$C_{OH} = \frac{2S_{HO_x} - S_{HO_2}}{2[OH]_0} \quad (5)$$

$$C_{HO_2} = \frac{S_{HO_2}}{2[OH]_0} \quad (6)$$

$$C_{RO_2} = \frac{2S_{RO_x} - S_{HO_2}(1+\delta)}{2[OH]_0(1-\delta)} \quad (7)$$

In a simple model, the sensitivities C_i can be expressed as a product of three generic parameters:

$$C_i = \gamma_i \epsilon_i \beta_{OH} \qquad \text{with} \quad i = OH, HO_2, RO_2 \quad (8)$$

γ_i represents the fraction of radical species i that are transmitted through the instrument inlet. ϵ_i denotes the yield of OH after the sampled radical species i has passed the distance from the gas inlet (nozzle) to the detection volume, and β_{OH} is the internal detection efficiency of OH in the detection volume. Among these parameters, ϵ_i and β_{OH} are influenced by the injected NO. More specifically, ϵ_i accounts for NO-dependent Reactions (R1) to (R5), which determine the fraction of OH that reaches the detection volume. ϵ_i represents the loss of OH by HONO formation for sampled OH (Reaction R2), while it represents the efficiency of chemical conversion to OH for sampled peroxy radicals. In principle, β_{OH} is influenced by NO-dependent quenching of the OH fluorescence, but this effect is small for the NO concentrations used in this work.

4 Experimental results for detection sensitivities

4.1 OH and HO_2 detection sensitivities

In order to investigate the HO_2 and OH detection sensitivities, the instrument sampled from the calibration source in the HO_2- and HO_x-mode of the radical source. We define

AMTD
4, 1255–1302, 2011

the relative HO_2 detection sensitivity of the instrument, α_{HO_2}, as the ratio of the calibration factors for HO_2 and OH (Eq. 8) that can be calculated from measurements using Eqs. (5) and (6). This gives the HO_2 conversion efficiency weighted by the ratio of the inlet transmission efficiencies for HO_2 and OH:

$$\alpha_{HO_2} = \frac{C_{HO_2}}{C_{OH}} = \frac{\gamma_{HO_2}}{\gamma_{OH}} \frac{\epsilon_{HO_2}}{\epsilon_{OH}} \quad (9)$$

Furthermore, we determine the influence of NO on the OH detection sensitivity as:

$$\epsilon_{OH} = \frac{C_{OH}(NO)}{C_{OH}(NO = 0)} \quad (10)$$

Figure 3 shows α_{HO_2} (upper panel) and ϵ_{OH} (lower panel) depending on the NO concentration for the two different inlet nozzles (reaction times) tested here. For high NO concentrations relative detection sensitivities are approximately constant at a value larger than one. The dashed vertical line in Fig. 3 indicates the NO concentration, at which the LIF instrument (with the 0.4 mm nozzle) was operated during field campaigns in the past. Measurements show that the HO_2 conversion in the detection is nearly complete for this NO concentration.

The OH sensitivity, which is shown in the lower panel of Fig. 3, is nearly independent of the NO concentration within the range tested here and decreases only slightly for large NO concentrations.

4.2 RO_2 detection sensitivities

The potential for an OH signal caused by the conversion of RO_2 to HO_2 via Reactions (R3) and (R4) and subsequent conversion to OH is investigated for various RO_2 radicals. Like for HO_2 we define the relative RO_2 detection sensitivity as the ratio of calibration factors for RO_2 and HO_2 (Eq. 8), which can be calculated from measurements using Eqs. (7) and (6):

AMTD
4, 1255–1302, 2011

$$\alpha_{RO_2} = \frac{C_{RO_2}}{C_{HO_2}} = \frac{\gamma_{RO_2}}{\gamma_{HO_2}} \frac{\epsilon_{RO_2}}{\epsilon_{HO_2}} \quad (11)$$

The experimental determination of the relative RO_2 detection sensitivity is only possible, if the yield of prompt HO_2 is known (δ in Eq. 7). α_{RO_2} represents the value of the interference from RO_2 radicals. It always refers to the HO_2 detection sensitivity of the instrument that is achieved for the same operational conditions.

In this work, values for the relative detection sensitivity for various peroxy radicals were determined. Results are summarized in Table 2 and examples of the measurements are shown in Fig. 4 for methane, Fig. 5 for isoprene and Fig. 6 for benzene.

Alkyl peroxy radicals are produced by the reaction of an alkane with OH in the radical source. Initial H-atom abstraction is followed by the reaction of the alkyl radical with O_2 (Atkinson and Arey, 2003) producing alkyl peroxy radicals. The relative detection sensitivity for methyl peroxy radicals, which are produced in the reaction of methane with OH, is below the limit of detection of the instrument for the configuration of the instrument with the 0.2 mm nozzle for the range of NO concentration tested here (open circles in Fig. 4). For the larger orifice, however, a small interference of 0.04 ± 0.04 is measured for the NO concentration, at which the cell was operated in the field (filled circle at dashed vertical line). Measurements exhibit a maximum of nearly 0.1 at smaller NO concentrations. This behavior was reproduced in several experiments.

Relative detection sensitivities are investigated for two other alkyl peroxy radicals, ethyl peroxy and cyclohexyl peroxy radicals, from the reaction of OH with ethane and cyclohexane, respectively, for two configurations of the detection cell (Table 2). For the configuration using the 0.4 mm orifice, the relative detection sensitivity of 0.07 ± 0.03 is small for ethyl peroxy radicals, but it is significantly larger for cyclohexyl peroxy radicals (0.48 ± 0.14). It is reduced to values within the range of the limit of detection of the instrument for the configuration with the 0.2 mm orifice for both radical species.

The major pathway of the reaction of OH with alkenes is its addition to the carbon atoms of the double-bond forming a β-hydroxyalkyl radical, which then reacts with O_2 to

AMTD
4, 1255–1302, 2011

form the corresponding β-hydroxyalkyl peroxy radical (Atkinson and Arey, 2003). Relative detection sensitivities were measured for radicals for the peroxy radicals from the OH reaction with ethene, propene and isoprene. All of them show a high relative detection sensitivity (Table 2) for the configuration with the 0.4 mm nozzle with 0.85 ± 0.05, 0.95 ± 0.03 and 0.79 ± 0.05 for radicals from ethene, propene and isoprene, respectively. The values are significantly reduced (0.17 ± 0.03, 0.15 ± 0.03 and 0.12 ± 0.02) for the configuration with the 0.2 mm nozzle. Figure 5 shows the dependence of the relative detection sensitivity on the NO concentration in the detection cell for RO_2 radicals from isoprene plus OH, emphasizing the NO dependence of the relative detection sensitivity. The high relative detection sensitivities suggest a fast conversion of β-hydroxyalkoxy radicals to HO_2. This means that RO_2 radicals from isoprene produced a strong interference signal for HO_2 measurements by the LIF-instrument in the past.

Relative detection sensitivities for RO_2 radicals from MVK and MACR are shown in Table 2. They are smaller than that measured for ethene and propene for the configuration used in field campaigns (0.4 mm nozzle), but are still significant (MVK: 0.60 ± 0.06, MACR: 0.58 ± 0.04). They are reduced to values within the range of values for other alkenes (MVK: 0.24 ± 0.11, MACR: 0.14 ± 0.02), if the smaller orifice (shorter reaction time) is used.

The reaction of benzene with OH is an example for prompt formation of HO_2 within the transport time of the calibration gas in the radical source ($\delta > 0$ in Eq. 7). The formation of HO_2 in air is fast (2.2 ms) (Bohn and Zetzsch, 1999), much shorter than the travel time of air between photolysis and sampling by the instrument. A yield of 65% recommended in literature based on product studies in the EUPHORE chamber (Bloss et al., 2005a,b) is taken for calculations using Eq. (7). We investigated recently the yield of prompt HO_2 formation by directly observing the HO_2 formation (Nehr et al., 2011). Here, the relative detection sensitivity for RO_2 radicals from benzene plus OH was found to be approximately 0.9 for high NO concentrations for the two configurations with the different inlet nozzles (Fig. 6). It is approximately 0.85 at the working point of the 0.4 mm nozzle used in previous field campaigns. The relative detection sensitivity

AMTD
4, 1255–1302, 2011

decreases with decreasing NO concentration and is smaller than 0.1 for the 0.2 mm nozzle at the lowest NO concentration tested here.

4.3 Water dependence of HO_2 and RO_2 detection sensitivities

The measurement intercomparison for HO_2 by different LIF instruments during HOxCOMP revealed discrepancies that were apparently correlated with the atmospheric water vapor (Fuchs et al., 2010). This result was surprising, because all instruments had corrected their measurements for the known influence of OH fluorescence quenching by water vapor. Results from this campaign must therefore be considered as a hint to a so far unknown water-related interference. For this reason, the water vapor dependence of our LIF detection sensitivity for HO_2 was reinvestigated (Fig. 7).

In the upper panels, the calibration factors for HO_2 and RO_2 are shown, both of which decrease with increasing water vapor concentration in the same way. The trend is compared to calculations that give the reduction of the sensitivity due to fluorescence quenching by water vapor using quenching constants from literature (Heard and Henderson, 2000). Calculations and measurements are in good agreement. This proves once more that the correction factor that was applied to measurements from this LIF instrument during HOxCOMP accounts for a dependence of the instrument sensitivity correctly. The relative detection sensitivity for the isoprene peroxy radicals does not show any significant trend with the water vapor mixing ratio for both inlet nozzles. This suggests that water vapor does not influence the overall RO_2 to OH conversion at the conditions in our measurement instrument.

AMTD
4, 1255–1302, 2011

5 Discussion of detection sensitivities

5.1 OH and HO_2 detection sensitivities of the LIF instrument

The relative detection sensitivities for HO_2 increases with NO and is approximately constant for high NO. In this case, the HO_2 conversion to OH is complete ($\frac{\epsilon_{HO_2}}{\epsilon_{OH}} \rightarrow 1$ in Eq. 9). The plateau value has a value of greater than one (Fig. 3, upper panel), which can be explained by different transmission efficiencies for HO_2 and OH (Eq. 9). The HO_2 inlet transmission efficiency is approximately 45% larger than that for OH for the 0.2 mm nozzle and 15% larger for the 0.4 mm nozzle. A larger inlet transmission efficiency for HO_2 than for OH is expected because of the generally smaller reactivity of HO_2 towards surfaces (Mihele and Hastie, 1998; Fuchs et al., 2008).

Measured α_{RO_2} values are compared to calculated values using the framework of the Master Chemical Mechanism version 3.1 (MCMv3.1, Saunders et al., 2003; Jenkin et al., 2003), in order to simulate the radical conversion. The initial concentration of HO_2 is set to 1×10^8 cm^{-3} for model calculations. The ratio of the calculated OH concentration after the reaction time, which is determined as described below, and the initial HO_2 concentration gives the HO_2 conversion efficiency ϵ_{HO_2} in Eqs. (8) and (9). The ratio of inlet transmission efficiencies determined for measurements at high NO concentrations is used to scale the results of model calculations, since the model does not include inlet loss reactions.

The reaction time for radical conversion in the detection cell is determined by fitting the modeled HO_2 curve to the measured data in Fig. 3, upper panel. This reaction time is used as model input for all other model calculations. A reaction time of 0.18 ± 0.025 ms for the 0.2 mm nozzle and a reaction time of 2.7 ± 0.5 ms for the 0.4 mm nozzle is determined (errors are estimated from sensitivity runs). The value for the 0.2 mm nozzle is similar to previous results (Weber, 1998), but the reaction time for the 0.4 mm nozzle is much longer. Air is sampled by supersonic expansion in both cases, so that similar travel times in the detection cell may be expected.

AMTD
4, 1255–1302, 2011

Model calculations reproduce the NO dependence of the measured relative HO_2 detection sensitivities (Fig. 3). Also the NO dependence of the OH detection efficiency (Fig. 3, lower panel) is well-described. The small decrease at high NO concentrations can be explained by OH loss in its reaction with NO forming HONO (Reaction R2).

The sampled air cools down significantly when it is expanded from ambient pressure to the low pressure in the measurement instrument. Previous experiments with a nozzle orifice of 0.75 mm showed a large reduction of the rotational temperature of OH in the probing laser beam to $T = 207$ K (Holland et al., 1995). When an orifice diameter of 0.2 mm or 0.4 mm is used, the rotational temperature is found to be equal to room temperature indicating that the expanded gas has come into thermal equilibrium with the surrounding sheath gas, when it reaches the laser beam. In order to estimate the influence of a temperature gradient on the peroxy radical conversion along the line from the NO injection point to the detection volume, we have also performed model calculations at a reduced temperature of 230 K. The difference to model results for 295 K is small (< 20%). This is also the case for all other model calculations that are performed, in order to calculate RO_2 conversion efficiencies below, indicating a negligible effect of temperature on the conversion reaction schemes (as far as they are known and included in MCMv3.1).

5.2 Interference from alkyl peroxy radicals

The high NO concentration in the detection cell ensures that alkyl peroxy radicals react exclusively with NO forming alkoxy radicals (Reaction R3). The rate constant of this reaction is similar for different RO_2 (typically 9×10^{-12} cm^{-3}s^{-1} at 298 K) (Atkinson and Arey, 2003). In addition to alkoxy radicals alkyl nitrates can be formed, but their yield is not well-known (Atkinson and Arey, 2003). Studies show that the yield is increasing with increasing number of C-atoms in the peroxy radical and with increasing pressure (Atkinson and Arey, 2003; Zhang et al., 2004). The lifetime of peroxy radicals is approximately 1 ms for conditions, at which the detection cell was operated in the field (0.4 mm nozzle, [NO] = 1.3×10^{14} cm^{-3}). Therefore, a substantial part of the alkyl

AMTD
4, 1255–1302, 2011

peroxy radicals can be converted to alkoxy radicals within the reaction time determined from investigations of the HO_2 conversion efficiency (2.7 ms). Alkoxy radicals react via one or more pathways (Atkinson, 1997b; Orlando et al., 2003): (1) Reaction with oxygen, (2) decomposition, (3) isomerization, (4) reaction with NO.

Model calculations (Fig. 4) that were performed to calculate the RO_2 conversion efficiency for methyl peroxy radicals agree with measurements for the short reaction time of the 0.2 mm nozzle showing that RO_2 conversion is negligible. For the longer reaction time with the 0.4 mm nozzle model calculations predict an increase of the RO_2 conversion efficiency with increasing NO concentrations, because of the faster conversion to HO_2. The small maximum in the measured RO_2 detection sensitivities at lower NO cannot be reproduced by model calculations using one reaction time. The reason for the discrepancy between measurements and model calculation is not clear. One may speculate that part of the sampled gas has a much longer residence time than determined from measurements of the HO_2 conversion efficiency due to e.g. recirculation in the background volume of the detection cell, so that a description of measurements with a single reaction time may not be sufficient. However, since CH_3O_2 is the most prominent radical for a wide range of atmospheric conditions, the important point is that there is no significant interference from methyl peroxy radicals for conditions at which the instrument was operated in the past.

The relative detection sensitivity for larger alkyl peroxy radicals may be greater than that for methyl peroxy radicals, since the reaction of alkoxy radicals, formed in the reaction of alkyl peroxy radicals with NO, with O_2 is faster by a factor of 4 to 6 (Atkinson and Arey, 2003; Orlando et al., 2003). Again, neither reaction rate constants nor the importance of decomposition and isomerization are well-known. Model calculations of the conversion efficiency for ethyl peroxy and cyclohexyl peroxy radicals approximately agree with measurements (Table 2). A larger discrepancy is only observed for cyclohexyl peroxy radicals, when the 0.4 mm nozzle is used. A large relative detection sensitivity of 0.48 ± 0.14 is measured, but model calculations predict only a small conversion efficiency of 0.14. This may be due to fast production of HO_2 from decomposition of

AMTD
4, 1255–1302, 2011

the cyclohexoxy radical that competes with the ring maintaining reaction with O_2 (Aschmann et al., 1997; Orlando et al., 2000), but HO_2 production from this reaction has not been investigated so far. The yield of other ring-opening decomposition products was estimated to be nearly 0.50 for atmospheric conditions (Aschmann et al., 1997) similar to the relative conversion efficiency measured here. MCMv3.1 lacks any decomposition of the cyclohexoxy radical, so that it is not expected that the calculated conversion efficiency of the cyclohexyl radical agrees with measurements.

Results obtained here agree with previous investigations for our LIF instrument (Weber, 1998; Holland et al., 2003). An upper limit for an interference from methyl peroxy radicals of 0.05 was measured using the 0.2 mm nozzle. Potential interferences from small alkyl peroxy radicals in the HO_2 detection were also investigated for other LIF instruments and found to be negligible in agreement with results obtained here. Kanaya et al. (2001) investigated the detection sensitivity of an LIF instrument for ethyl peroxy radicals. A relative detection sensitivity of 0.05 was found. The potential for interferences from C_1–C_4 alkyl peroxy radicals were also experimentally investigated for another LIF instrument by Ren et al. (2004) and found to be negligible.

5.3 Interference from β-hydroxyalkyl peroxy radicals

Similar to alkyl peroxy radicals, β-hydroxyalkyl peroxy radicals can undergo conversion reactions leading finally to the formation of HO_2 in the detection cell. As an example, Fig. 8 shows the reaction sequence for β-hydroxyalkyl peroxy radical from ethene plus OH. They react with NO forming β-hydroxyalkoxy radicals with a reaction rate constant that is similar to those of alkyl peroxy radicals (Atkinson and Arey, 2003). β-hydroxyalkoxy radicals can react with O_2 or can decompose or isomerize. However, in contrast to alkoxy peroxy radicals, decomposition and isomerization appear to be the dominant pathways, except for the $HOCH_2CH_2O$ radical (from ethene plus OH), for which decomposition and reaction with O_2 can be competitive (Atkinson, 1997a). Decomposition rate constants were determined to be on the order of 10^4 to 10^6 s^{-1} (Atkinson, 1997a,b; Orlando et al., 1998; Vereecken et al., 1999). Decomposition leads to the

AMTD
4, 1255–1302, 2011

formation of a hydroxyalkyl radical, which then reacts rapidly and solely with O_2 forming a carbonyl compound plus HO_2 (Atkinson, 1997b; Orlando et al., 2003). Compared to the slow alkoxy + O_2 reaction (e.g., for CH_3O), which inhibits the overall RO_2 to OH conversion for simple alkyl peroxy radicals in our detection cell, decomposition of β-hydroxyalkoxy radicals is extremely fast. Therefore, the lifetime of the β-hydroxyalkoxy radical is much shorter than the reaction time in the detection cell for the 0.4 mm nozzle, so that they are efficiently converted to HO_2. As a consequence, the reaction with NO limits the conversion efficiency, so that a strong interference is observed for high NO concentrations that decreases with decreasing NO in contrast to assumption made in the past.

In the MCMv3.1 decomposition of the β-hydroxyalkoxy radical is lumped with the subsequent reaction of the hydroxyalkyl radical with O_2. Due to the reduced density of O_2 in the detection cell, calculations using MCMv3.1 may not accurately describe the conversion efficiency. In addition, inlet transmission efficiencies for β-hydroxyalkyl peroxy radicals may be different from that for HO_2. Despite these limitations calculated conversion efficiencies approximately match relative detection sensitivities as shown in Table 2).

5.4 Interference from RO_2 produced by isoprene + OH and its oxidation products + OH

The fate of peroxy radicals from isoprene and OH is subject of recent theoretical and experimental investigations (Peeters et al., 2009; da Silva et al., 2010). If NO is present, the reaction pathway is similar to that of an alkene, but four different hydroxyalkyl peroxy radicals can be formed (Fan and Zhang, 2004; Ghosh et al., 2010; Greenwald et al., 2010), two of which are favored (yield: 0.97). They can be converted to HO_2 in a radical reaction sequence. Peeters et al. (2009) suggest that the hydroxyalkyl peroxy radical may also undergo a 1,6-H-shift with subsequent decomposition and formation of HO_2 instead of reaction with NO. This prompt HO_2 formation may be of importance under low NO conditions. Another theoretical study by da Silva et al. (2010) suggests a high

AMTD
4, 1255–1302, 2011

yield of HO_2 from unimolecular decomposition of the hydroxyalkyl peroxy radical to HO_2 in the absence of NO. No NO is present in the radical source, so that these reaction pathways would change the ratio of RO_2 to HO_2 towards HO_2 (Eq. 7 with $\delta > 0$).

Lines in Fig. 5 show relative conversion efficiencies of RO_2 radicals from isoprene to HO_2 from model calculations using MCMv3.1, which does not include the recently suggested prompt HO_2 formation from the hydroxyalkyl peroxy radical. Conversion efficiencies of the four peroxy radicals that are formed in the reaction of isoprene with OH are weighted averages with weights accounting for the formation yields of the peroxy radical species assumed in MCMv3.1. Although the reaction mechanism neglects details of the conversion of the hydroxyalkoxy radicals to HO_2, calculations reproduce roughly the observations. The agreement is better for the 0.2 mm nozzle, whereas measurements seem to be shifted towards smaller NO concentrations for the 0.4 mm nozzle. However, one has to keep in mind that calculated conversion efficiencies need to be weighted by the ratio of the inlet transmission efficiencies for RO_2 and HO_2 to be compared to measured relative detection sensitivities (Eq. 11). They are approximately 10% larger for the 0.4 mm nozzle at high NO concentrations than calculated conversion efficiencies. This indicates that inlet transmission efficiency for peroxy radicals from isoprene may be slightly larger than that for HO_2 for this nozzle. Moreover, results for methyl peroxy radicals indicates (see above) that the description of the RO_2 conversion with one reaction time may not be sufficient.

Measured relative detection sensitivities are larger than calculated conversion efficiencies at low NO concentrations for both inlet nozzles. The difference of 0.08 can be regarded as an upper limit for potential prompt HO_2 formation (Eq. 11) in the radical source as suggested by Peeters et al. (2009) and da Silva et al. (2010) within the time between formation and detection of RO_2 radicals (20 ms). This upper limit would be consistent with the limit of the rate constant for the 1,6-H-shift given by Peeters et al. (2009), which converts to a lifetime of 120 ms, but does not fit to results obtained by Nehr et al. (2011), who investigated prompt HO_2 formation on a time scale of one second. However, the same authors lowered recently the estimate for the rate constant to

AMTD
4, 1255–1302, 2011

$0.1\,s^{-1}$ (Peeters and Muller, 2010). In this case, the 1,6-H-shift would be too slow to be observed in experiments conducted here. The decomposition rate given by da Silva et al. (2010) for direct decomposition of the hydroxyalkyl peroxy radical (lifetime of several minutes) is too small to play a role in these experiments.

The two major atmospheric oxidation products from the degradation of isoprene with OH are MVK and MACR, both of which can be further oxidized by OH. The fate of RO_2 radicals from MVK and MACR plus OH are not well-known. Like for alkenes OH can add to the C = C double bond at two positions for MVK, so that two hydroxyalkyl peroxy radical species are formed. Both react with NO forming hydroxyalkoxy radicals, which further decompose. The hydroxyalkoxy radical that is formed, if OH adds at the terminal CH_2 group of MVK (yield: 0.64), decomposes via two channels (Tuazon and Atkinson, 1989), so that three conversion paths are possible. Two of them are similar to the reaction chain that follows the path described above for alkenes, so that a fast conversion to HO_2 is possible. However, decomposition products of the third channel do not lead to a fast HO_2 production. For this reaction path Tuazon and Atkinson (1989) measured a yield of 0.64 (referred to the entire reaction of MVK from product studies). Consequently, only the remaining part (36%) can lead to a fast conversion of RO_2 to HO_2 in the detection cell via the other two reaction channels. The relative detection sensitivity for RO_2 radicals is significantly larger (0.60) inconsistent with this reaction scheme. Calculations using MCMv3.1 (Table 2) give even smaller conversion efficiencies, since the mechanism does not include all of the conversion paths that lead to fast formation of HO_2.

In contrast to MVK, OH can add to MACR (yield: 0.43) or can abstract an H-atom (yield: 0.57) (Tuazon and Atkinson, 1990; Orlando et al., 1999). H-abstraction leads to the formation of an acyl peroxy radical that reacts with NO to the 1-methylvinyl radical and cannot be converted to HO_2 within the reaction time in the HO_2 detection cell. The hydroxyalkyl peroxy radical that is formed, if OH adds to MACR, follows the reaction path of other hydroxyalkyl peroxy radicals, so that HO_2 is formed quickly. Therefore, it is reasonable that the relative detection sensitivity for peroxy radicals (0.58 ± 0.04,

AMTD
4, 1255–1302, 2011

Table 2) from the reaction of MACR with OH for the configuration with the 0.4 mm nozzle is within the range of the yield of hydroxyalkyl peroxy radicals (0.43) (Tuazon and Atkinson, 1990; Orlando et al., 1999). Also calculations of the conversion efficiency using MCMv3.1 (Table 2) give a relative RO_2 conversion efficiency that is similar to the yield of hydroxyalkyl peroxy radicals for this configuration.

5.5 Interference from RO_2 produced by benzene + OH

Measured detection sensitivities for RO_2 from benzene plus OH agrees approximately with calculated conversion efficiencies using MCMv3.1. Equations (7) and (11) with $\delta = 0.65$ are used to determine the relative detection sensitivity, so that prompt HO_2 formation in the radical source does not add to the relative detection sensitivity of the peroxy radical. Error bars of data are relatively large (Fig. 6), because of the small RO_2 concentration compared to HO_2 from prompt HO_2 formation in the radical source.

OH adds to benzene forming the hydroxycyclohexadienyl radical, which reacts predominantly with O_2 in air (Nehr et al., 2011). Products are phenol plus HO_2 (yield: 0.53, Volkamer et al., 2002) and RO_2 radicals, part of which most likely decomposes to epoxides and HO_2 (yield: 0.12, Bloss et al., 2005b). Only 0.35 of the products in the reaction of benzene with OH is a bicyclic peroxy radical which behaves similar to hydroxyalkyl peroxy radicals. After reaction with NO products decompose and react with O_2 yielding HO_2 very fast, so that the first reaction step becomes limiting to the conversion efficiency in the HO_2 detection cell. Therefore, the RO_2 radical species from benzene plus OH can be an interference for HO_2 measurements for conditions at which RO_2 radicals from alkene plus OH interfere.

AMTD
4, 1255–1302, 2011

6 Implication for atmospheric HO_2 concentration measurements by LIF

Investigation of relative detection sensitivities of the LIF instrument described in the previous section show that RO_2 can be a significant interference for HO_2 concentration measurements. Experiments indicate that a large fraction of RO_2 radicals from alkene plus OH reactions including isoprene and from aromatics plus OH reactions are detected for conditions, at which the instrument was operated during field campaigns in the past. Interferences from RO_2 radicals identified here (mostly β-hydroxyalkyl peroxy radicals), can be significantly reduced, if the NO concentration and/or the reaction time in the detection cell is decreased. Although the HO_2 detection sensitivity becomes smaller at the same time, operation of the instrument at lower NO concentration and with shorter reaction time is feasible. In this case, the HO_2 sensitivity is only reduced by a factor of four (Fig. 3), but the relative RO_2 sensitivity is smaller than 0.2 for most of RO_2 species studied here (Table 2). This value for the HO_2 sensitivity will be still sufficient for detecting HO_2 for a wide range of conditions in the atmosphere.

HO_2 measurements that we performed with our LIF instrument in past field campaigns and in simulation chamber experiments need to be revised, depending on the abundance and mix of RO_2 species present during the distinct campaigns. The interference by RO_2 is generally expected to be negligible for remote and marine environments, where methyl peroxy radicals are the dominant RO_2 species. However, significant interferences in HO_2 measurements are expected in the presence of high concentrations of alkenes and aromatics, as is typically found in urban and forested environments. In principle, speciated RO_2 measurements are required to correct for the interference, but such measurements do not exist. A detailed analysis of the consequences for past field measurements is beyond the scope of this paper and will be discussed elsewhere. For example, a significant impact of the interference is expected for the recently published HO_x measurements performed during the PRIDE-PRD2006 campaign in the Pearl River Delta, China (Hofzumahaus et al., 2009). Model calculations suggest that the measured HO_2 concentrations contain an interference by RO_2

AMTD
4, 1255–1302, 2011

of at least 30% during daytime, depending on the chemical mechanism used for the calculation of the RO_2 species (Lu et al., 2011). This also suggests that the unknown radical recycling, proposed by Hofzumahaus et al. (2009) to explain the observed OH, must be even larger, if the HO_2 concentrations are smaller than assumed before (Lu et al., 2011).

An LIF instrument similar to the one for HO_2 detection was recently developed for alternating measurement of HO_x and RO_x radicals (Fuchs et al., 2008). This instrument utilizes the conversion of RO_2 radicals to HO_2 as described above (Reactions R3, R4) in an additional conversion reactor that is mounted on top of a detection cell that is similar to the HO_2 detection cell characterized here. The sum of OH, HO_2 and RO_2 is converted to HO_2 in the conversion reactor in the RO_x-mode of the system. The RO_2 conversion efficiency in the reactor is mainly determined by the rate constant of the reaction of RO_2 with NO, so that effects described here, do not impact RO_x measurements. However, since conditions were chosen for a high HO_2 conversion efficiency in the HO_2 detection cell downstream of the conversion reactor, HO_2 concentration measurements in the HO_x-mode of the instrument are affected by similar RO_2 interferences as described above. In the HO_2 measurement mode RO_2 radicals are not converted in the conversion reactor, but can be converted to OH in the HO_2 detection cell as shown above. Therefore, the instrument is not sufficiently capable of separating between HO_2 and RO_2 radicals from alkenes and aromatics. In the future, it is planned to install a separate HO_2 detection cell, which will be operated at optimized conditions (low NO concentration and shorter reaction time). This will allow separating HO_2 and RO_2 radical concentrations by subtracting the signals of the RO_x- and HO_x-channel of the instrument. HO_2 comparison measurements of ROxLIF with measurements by MIESR in the past (Fuchs et al., 2009) is expected to be unaffected by interferences from RO_2, because only methyl peroxy radicals and ethyl peroxy radicals, which are not efficiently converted in the HO_2 detection cell, were involved. This expectation is consistent with the good correlation and absolute agreement between HO_2 and RO_2 concentration measurements of both instruments observed for the two techniques.

AMTD
4, 1255–1302, 2011

Although NO concentrations and reaction times in the detection cell are different for other LIF instruments, it is likely that these instruments also suffer from the interferences discovered here. All LIF-instruments make use of the conversion of HO_2 via reaction with NO reach HO_2 conversion efficiencies that are greater than 0.9 (Heard and Pilling, 2003). As shown above, the HO_2 conversion efficiency is closely connected to the RO_2 conversion efficiency for RO_2 species from alkene- and aromatic-precursors and can reach similar values for large NO concentrations.

HO_2 concentration measurements of three LIF instruments were compared during the HOxCOMP campaign in 2005 (Fuchs et al., 2010). Measurements were partly conducted in ambient air and partly at the atmosphere simulation chamber SAPHIR. Since the measurement place was influenced by biogenic emissions, most likely RO_2 radicals from isoprene and its reaction products were present during ambient air sampling and may have corrupted HO_2 concentrations that were reported for the three instruments. However, the interference would likely appear in a difference in the slope from unity in the correlation plot rather than in an offset for two reasons: (1) HO_2 and RO_2 concentrations are often highly correlated (Mihelcic et al., 2003), (2) measurements of all instruments were most likely affected in a similar way. Thus, the interference would not be distinguishable from calibration errors. This is also the case for those experiments in SAPHIR during which RO_2 radicals were produced. It is possible that some of the day-to-day variability observed in the slope of the correlation may have been caused by interferences from RO_2 radicals. However, half of the experiments in SAPHIR were conducted without the addition of organic compounds. Therefore, it is likely that major results of this campaign are not related to an interference from RO_2 radicals.

AMTD
4, 1255–1302, 2011

7 Summary and conclusions

HO_2 concentration measurements are widely accomplished by chemical conversion of HO_2 to OH including reaction with NO and subsequent detection of OH by laser-induced fluorescence. RO_2 radicals can be converted to OH via a similar radical reaction sequence including reaction with NO, so that they are potential interferences for HO_2 measurements. It was believed that this reaction path does not play a role for LIF instruments. Here, RO_2 detection sensitivities relative to that for HO_2 were measured for RO_2 radicals from various organic precursors such as alkanes, alkenes including isoprene and aromatics. They were produced by the reaction of VOCs with OH in a radical source that produces OH and HO_2 by water photolysis. The ratio of OH and HO_2 concentrations in the radical source were determined in a separate experiment, in order to avoid uncertainties from potential discrepancies of the ratio from unity. Major results of these investigations are:

- The ratio of HO_2 to the sum of HO_2 and OH concentrations produced by water photolysis at 185 mm in air is 0.50 ± 0.02.
- The interference of HO_2 measurements from RO_2 produced by the reaction of OH with small alkanes via H-atom abstraction is within the range of a few percent for the LIF instrument operated at conditions used in field campaigns in the past in agreement with results reported from other groups.
- The interference from RO_2 from OH plus alkenes or aromatics (OH-addition) is larger than 0.8 for the LIF instrument operated with these conditions.
- Interferences from RO_2 radicals produced by the reaction of isoprene and its oxidation products, MVK and MACR, with OH are 0.8 and 0.6, respectively, for the LIF instrument operated with these conditions.
- The reaction of RO_2 with NO limits the conversion efficiency for interfering RO_2 radical species in contrast to assumptions made in the past that the reaction of

AMTD
4, 1255–1302, 2011

alkoxy radicals with O_2 suppresses the conversion. This is due to the fast reaction of β-hydroxyalkoxy radicals with O_2.

– Interferences from these RO_2 species can be significantly reduced (< 0.2), if the reaction time and/or the NO concentration in the detection cell is reduced on the cost of a reduced HO_2 detection sensitivity.

Consequently, HO_2 concentration measurements from previous field campaigns during which this LIF instrument was deployed give rather the sum of HO_2 and some fraction of RO_2 than HO_2 alone. Generally, the interference by RO_2 radicals would be small in clean remote environments, when small alkanes dominate the OH reactivity, but would be most likely larger in polluted environments. This is also the case for areas that have large biogenic emissions, because RO_2 radicals from isoprene and its oxidation products are efficiently converted in the detection cell. The impact of interferences from RO_2 is highest, if the oxidation rate of pollutants such as alkenes including isoprene is high (high VOC and OH concentrations) but NO concentrations are small as found e.g. during the PRIDE-PRD2006 campaign (Lu et al., 2011). For this campaign, model calculations suggest that the measured HO_2 concentrations contain an interference by RO_2 of at least 30% during daytime. The unknown radical recycling, proposed by Hofzumahaus et al. (2009) to explain the observed OH, however, must be even larger, if the OH source from HO_2 is smaller than assumed before.

Results of investigations done here implicate that the detection of HO_2 via chemical conversion with NO and subsequent detection of OH needs to be revisited. Running the LIF instrument at much lower NO concentration and/or shorter reaction time for HO_2 to OH conversion will provide a significantly improved suppression of interferences from RO_2 (less than 0.2). Although the HO_2 sensitivity of the instrument will be reduced at the same time, this should allow useful studies of the atmospheric chemistry at most tropospheric conditions. Further characterization of interferences for a wider range of RO_2 species and redesign of the instrument may be required, in order to minimize interferences from RO_2 radicals.

AMTD
4, 1255–1302, 2011

References

Andrés-Hernández, M. D., Stone, D., Brookes, D. M., Commane, R., Reeves, C. E., Huntrieser, H., Heard, D. E., Monks, P. S., Burrows, J. P., Schlager, H., Kartal, D., Evans, M. J., Floquet, C. F. A., Ingham, T., Methven, J., and Parker, A. E.: Peroxy radical partitioning during the AMMA radical intercomparison exercise, Atmos. Chem. Phys., 10, 10621–10638, doi:10.5194/acp-10-10621-2010, 2010. 1257

Aschmann, S. M., Chew, A. A., Arey, J., and Atkinson, R.: Products of the gas-phase reaction of OH radicals with cyclohexane: reactions of the cyclohexoxy radical, J. Phys. Chem. A, 101, 8042–8048, doi:10.1021/jp971869f, 1997. 1275

Aschmutat, U., Hessling, M., Holland, F., and Hofzumahaus, A.: A tunable source of hydroxyl (OH) and hydroperoxy (HO_2) radicals: in the range between 10^6 and $10^9\,cm^{-3}$, Physico-chemical behaviour of atmospheric pollutants, European Commission, Brussels, 1994. 1262

Atkinson, R.: Gase-phase tropospheric chemistry of volatile organic compounds: 1. Alkanes and alkenes, J. Phys. Chem. Ref. Data, 26, 217–290, 1997a. 1275

Atkinson, R.: Atmospheric reactions of alkoxy and β-hydroxyalkoxy radicals, Int. J. Chem. Kin., 29, 99–111, 1997b. 1274, 1275, 1276

Atkinson, R. and Arey, J.: Atmospheric degradation of volatile organic compounds, Chem. Rev., 103, 4605–4638, doi:10.1021/cr0206420, 2003. 1258, 1266, 1269, 1270, 1273, 1274, 1275

Bajeh, M. A., Goldfield, E. M., Hanf, A., Kappel, C., Meijer, A. J. H. M., Volpp, H.-R., and Wolfrum, J.: Dynamics of the $H + O_2 \rightarrow O + OH$ chain-branching reaction: accurate quantum mechanical and experimental absolute reaction cross sections, J. Phys. Chem. A, 105, 3359–3364, doi:10.1021/jp0036137, 2001. 1264

Bloss, C., Wagner, V., Bonzanini, A., Jenkin, M. E., Wirtz, K., Martin-Reviejo, M., and Pilling, M. J.: Evaluation of detailed aromatic mechanisms (MCMv3 and MCMv3.1) against environmental chamber data, Atmos. Chem. Phys., 5, 623–639, doi:10.5194/acp-5-623-2005, 2005a. 1270

Bloss, C., Wagner, V., Jenkin, M. E., Volkamer, R., Bloss, W. J., Lee, J. D., Heard, D. E., Wirtz, K., Martin-Reviejo, M., Rea, G., Wenger, J. C., and Pilling, M. J.: Development of a detailed chemical mechanism (MCMv3.1) for the atmospheric oxidation of aromatic hydrocarbons, Atmos. Chem. Phys., 5, 641–664, doi:10.5194/acp-5-641-2005, 2005. 1270, 1279

Bohn, B. and Zetzsch, C.: Gas-phase reaction of the OH-benzene adduct with O_2 : reversibility and secondary formation of HO_2, Phys. Chem. Chem. Phys., 1, 5097–5107, 1999. 1270

AMTD
4, 1255–1302, 2011

Burkert, J., Hernández, M. D. A., Stöbener, D., Weissenmayer, M., and Kraus, A.: Peroxy radical and related trace gas measurements in the boundary layer above the Atlantic Ocean, J. Geophys. Res., 106, 5457–5477, 2001. 1257

Cantrell, C. A., Stedman, D. H., and Wendel, G. J.: Measurement of atmospheric peroxy radicals by chemical amplification, Anal. Chem., 56, 1496–1502, 1984. 1257

Cantrell, C. A., Zimmer, A., and Tyndall, G. S.: Absorption cross sections for water vapor from 183 to 193 nm, Geophys. Res. Lett., 24, 2195–2198, 1997. 1263

Clemitshaw, K. C., Carpenter, L. J., and St, A. P.: A calibrated peroxy radical chemical amplifier for ground-based tropospheric measuerments, J. Geophys. Res., 102, 25405–25416, 1997. 1257

Creasey, D. J., Heard, D. E., and Lee, J. D.: Eastern Atlantic Spring Experiment 1997 (EASE97) 1. Measurements of OH and HO_2 concentrations at Mace Head, Ireland, J. Geophys. Res., 107, 4091, doi:10.1029/2001jd000892, 2002. 1259

Creasey, D. J., Evans, G. E., Heard, D. E., and Lee, J. D.: Measurements of OH and HO_2 concentrations in the Southern Ocean marine boundary layer, J. Geophys. Res., 108, 4475, doi:10.1029/2002JD003206, 2003. 1263

da Silva, G., Graham, C., and Wang, Z.-F.: Unimolecular β-hydroxyperoxy radical decomposition with OH recycling in the photochemical oxidation of isoprene, Environ Sci. Technol., 44, 250–256, doi:10.1021/es900924d, 2010. 1276, 1277, 1278

Dlugi, R., Berger, M., Zelger, M., Hofzumahaus, A., Siese, M., Holland, F., Wisthaler, A., Grabmer, W., Hansel, A., Koppmann, R., Kramm, G., Möllmann-Coers, M., and Knaps, A.: Turbulent exchange and segregation of HO_x radicals and volatile organic compounds above a deciduous forest, Atmos. Chem. Phys., 10, 6215–6235, doi:10.5194/acp-10-6215-2010, 2010. 1260

Edwards, G. D., Cantrell, C. A., Stephens, S., Hil, B., Goyea, O., Shetter, R. E., Mauldin, R. L., Kosciuch, E., Tanner, D. J., and Eisele, F. L.: Chemical ionization mass spectrometer instrument for the measurement of tropospheric HO_2 and RO_2, Anal. Chem., 75, 5318–5327, doi:10.1021/ac034402b, 2003. 1257, 1258, 1259

Engel, V., Staemmler, V., Vander Wal, R. L., Crim, F. F., Sension, R. J., Hudson, B., Andresen, P., Hennig, S., Weide, K., and Schinke, R.: Photodissociation of water in the first absorption band: a prototype for dissociation on a repulsive potential energy surface, J. Phys. Chem., 96, 3201–3213, doi:10.1021/j100187a007, 1992. 1263

AMTD
4, 1255–1302, 2011

Fan, J. and Zhang, R.: Atmospheric oxidation mechanism of isoprene, Environ. Chem., 1, 140–149, doi:10.1071/EN04045, 2004. 1276

Finlayson-Pitts, B. J. and Pitts Jr., J. N.: Chemistry of the Upper and Lower Atmosphere, Academic Press, San Diego, 2000. 1257

Fuchs, H., Hofzumahaus, A., and Holland, F.: Measurement of tropospheric RO_2 and HO_2 radicals by a laser-induced fluorescence instrument, Rev. Sci. Instrum., 79, 084104, doi:10.1063/1.2968712, 2008. 1258, 1265, 1272, 1281

Fuchs, H., Brauers, T., Häseler, R., Holland, F., Mihelcic, D., Müsgen, P., Rohrer, F., Wegener, R., and Hofzumahaus, A.: Intercomparison of peroxy radical measurements obtained at atmospheric conditions by laser-induced fluorescence and electron spin resonance spectroscopy, Atmos. Meas. Tech., 2, 55–64, doi:10.5194/amt-2-55-2009, 2009. 1260, 1281

Fuchs, H., Brauers, T., Dorn, H.-P., Harder, H., Häseler, R., Hofzumahaus, A., Holland, F., Kanaya, Y., Kajii, Y., Kubistin, D., Lou, S., Martinez, M., Miyamoto, K., Nishida, S., Rudolf, M., Schlosser, E., Wahner, A., Yoshino, A., and Schurath, U.: Technical Note: Formal blind intercomparison of HO_2 measurements in the atmosphere simulation chamber SAPHIR during the HOxComp campaign, Atmos. Chem. Phys., 10, 12233–12250, doi:10.5194/acp-10-12233-2010, 2010. 1259, 1260, 1271, 1282

Geyer, A., Bächmann, K., Hofzumahaus, A., Holland, F., Konrad, S., Klüpfel, T., Pätz, H. W., Schäfer, J., and Platt, U.: Nighttime formation of peroxy and hydroxyl radicals during the BERLIOZ campaign: observations and modeling studies, J. Geophys. Res., 108, 8249, doi:10.1029/2001JD000656, 2003. 1257

Ghosh, B., Bugarin, A., Connell, B. T., and North, S. W.: Isomer-selective study of the OH-initiated oxidation of isoprene in the presence of O_2 and NO: 2. The major OH addition channel, J. Phys. Chem. A, 114, 2553–2560, doi:10.1021/jp909052t, 2010. 1276

Green, T. J., Reeves, C. E., Fleming, Z. L., Brough, N., Rickard, A. R., Bandy, B. J., Monks, P. S., and Penkett, S. A.: An improved dual channel PERCA instrument for atmospheric measurements of peroxy radicals, J. Environ. Monitor., 8, 530–536, 2006. 1257

Greenwald, E. E., Ghosh, B., Anderson, K. C., Dooley, K. S., Zou, P., Selby, T., Osborn, D. L., Meloni, G., Taatjes, C. A., Goulay, F., and North, S. W.: Isomer-selective study of the OH initiated oxidation of isoprene in the presence of O_2 and NO, I. The minor inner OH-addition channel, J. Phys. Chem. A, 114, 904–912, doi:10.1021/jp908543a, 2010. 1276

AMTD
4, 1255–1302, 2011

Hanke, M., Uecker, J., Reiner, T., and Arnold, F.: Atmospheric peroxy radicals: ROXMAS, a new mass-spectrometric methodology for the speciated measurements of HO_2 and ΣRO_2 and first results, Int. J. Mass. Spectrom., 213, 91–99, 2002. 1257

Hard, T. M., O'Brian, R. J., Chan, C. Y., and Mehrabzadeh, A. A.: Tropospheric free radical determination by FAGE, Environ. Sci. Technol., 18, 768–777, 1984. 1260

Hastie, D. R., Weissenmayer, M., Burrows, J. P., and Harris, G. W.: Calibrated chemical amplifier for atmospheric RO_x measurements, Anal. Chem., 63, 2048–2057, 1991. 1257

Heard, D. E. and Henderson, D. A.: Quenching of $OH(A^2\Sigma^+, v' = 0)$ several collision partners between 200 and 344 K. Cross-section measurements and model comparisons, Phys. Chem. Chem. Phys., 2, 67–72, 2000. 1271

Heard, D. E. and Pilling, M. J.: Measurement of OH and HO_2 in the troposphere, Chem. Rev., 103, 5163–5198, doi:10.1021/cr020522s, 2003. 1257, 1259, 1260, 1262, 1282

Hofzumahaus, A., Aschmutat, U., Heßling, M., Holland, F., and Ehhalt, D. H.: The measurement of tropospheric OH radicals by laser-induced fluorescence spectroscopy during POPCORN field campaign, Geophys. Res. Lett., 23, 2541–2544, 1996. 1263

Hofzumahaus, A., Rohrer, F., Lu, K., Bohn, B., Brauers, T., Chang, C.-C., Fuchs, H., Holland, F., Kita, K., Kondo, Y., Li, X., Lou, S., Shao, M., Zeng, L., Wahner, A., and Zhang, Y.: Amplified trace gas removal in the troposphere, Science, 324, 1702–1704, doi:10.1126/science.1164566, 2009. 1257, 1260, 1280, 1281, 1284

Holland, F., Heßling, M., and Hofzumahaus, A.: In situ measurement of tropospheric OH radicals by laser-induced fluorescence – a description of the KFA instrument, J. Atmos. Sci., 52, 3393–3401, 1995. 1273

Holland, F., Hofzumahaus, A., Schäfer, J., Kraus, A., and Pätz, H. W.: Measurements of OH and HO_2 radical concentrations and photolysis frequencies during BERLIOZ, J. Geophys. Res., 108, 8246, doi:10.1029/2001JD001393, 2003. 1259, 1260, 1262, 1275

Hornbrook, R. S., Crawford, J. H., Edwards, G. D., Goyea, O., Mauldin III, R. L., Olson, J. S., and Cantrell, C. A.: Measurements of tropospheric HO_2 and RO_2 by oxygen dilution modulation and chemical ionization mass spectrometry, Atmos. Meas. Tech. Discuss., 4, 385–442, doi:10.5194/amtd-4-385-2011, 2011. 1257, 1259, 1265

Jenkin, M. E., Saunders, S. M., Wagner, V., and Pilling, M. J.: Protocol for the development of the Master Chemical Mechanism, MCM v3 (Part B): tropospheric degradation of aromatic volatile organic compounds, Atmos. Chem. Phys., 3, 181–193, doi:10.5194/acp-3-181-2003, 2003. 1272

AMTD
4, 1255–1302, 2011

Kanaya, Y., Sadanaga, Y., Nakamura, K., and Akimoto, H.: Development of a ground-based LIF instrument for measuring HO_x radicals: instrumentation and calibration, J. Atmos. Chem., 38, 73–110, 2001. 1259, 1275

Kanaya, Y., Cao, R., Akimoto, H., Fukuda, M., Komazaki, Y., Yokouchi, Y., Koike, M., Tanimoto, H., Takegawa, N., and Kondo, Y.: Urban photochemistry in central Tokyo: 1. observed and modeled OH and HO_2 radical concentrations during the winter and summer 2004, J. Geophys. Res., 112, D21312, doi:10.1029/2007JD008670, 2007. 1257

Kleffmann, J., Gavriloaiei, T., Hofzumahaus, A., Holland, F., Koppmann, R., Rupp, L., Schlosser, E., Siese, M., and Wahner, A.: Daytime formation of nitrous acid: a major source of OH radicals in a forest, Geophys. Res. Lett., 32, L05818, doi:10.1029/2005GL022524, 2005. 1260

Lelieveld, J., Butler, T. M., Crowley, J. N., Dillon, T. J., Fischer, H., Ganzeveld, L., Harder, H., Lawrence, M. G., Martinez, M., Taraborrelli, D., and Williams, J.: Atmospheric oxidation capacity sustained by a tropical forest, Nature, 452, 737–740, doi:10.1038/nature06870, 2008. 1257

Lu, K. D., Rohrer, F., Holland, F., Fuchs, H., Bohn, B., Brauers, T., Chang, C. C., Häseler, R., Hu, M., Kita, K., Kondo, Y., Li, X., Lou, S. R., Shao, M., Zeng, L. M., Wahner, A., Zhang, Y. H., and Hofzumahaus, A.: Observations of OH and HO_2 radicals in the Pearl River Delta in summer 2006: indications of intense photochemistry in southern China, in prep. for Atmos. Chem. Phys., 2011. 1260, 1281, 1284

Mather, J. H., Stevens, P. S., and Brune, W. H.: OH and HO_2 measurements using laser-induced fluorescence, J. Geophys. Res., 102, 6427–6436, 1997. 1259

Mihelcic, D., Müsgen, P., and Ehhalt, D. H.: An improved method of measuring tropospheric NO_2 and RO_2 by matrix isolation and electron spin resonance, J. Atmos. Chem., 3, 341–361, 1985. 1257

Mihelcic, D., Volz-Thomas, A., Pätz, H. W., Kley, D., and Mihelcic, M.: Numerical analysis of ESR spectra from atmospheric samples, J. Atmos. Chem., 11, 271–297, 1990. 1257

Mihelcic, D., Holland, F., Hofzumahaus, A., Hoppe, L., Müsgen, P., Pätz, H. W., and Moortgat, G. K.: Peroxy radicals during BERLIOZ at Pabstthum: measurements, radical budgets and ozone production, J. Geophys. Res., 108, 9–1, doi:10.1029/2001JD001014, 2003. 1282

Mihele, C. M. and Hastie, D. R.: The sensitivity of the radical amplifier to ambient water vapor, Geophys. Res. Lett., 25, 1911–1913, 1998. 1272

AMTD
4, 1255–1302, 2011

Mihele, C. M. and Hastie, D. R.: Optimized operation and calibration procedures for radical amplifyer-type detectors, J. Atmos. Ocean. Tech., 17, 788–794, 2000. 1257
Monks, P. S.: Gas-phase radical chemistry in the troposphere, Chem. Soc. Rev., 34, 376–395, doi:10.1039/b307982c, 2005. 1257
Nehr, S., Bohn, B., Fuchs, H., Hofzumahaus, A., and Wahner, A.: HO_2 formation from the OH + benzene reaction in the presence of O_2, Phys. Chem. Chem. Phys., submitted, 2011. 1266, 1270, 1277, 1279
Orlando, J. J., Tyndall, G. S., Bilde, M., Ferronato, C., Wallington, T. J., Vereecken, L., and Peeters, J.: Laboratory and theoretical study of the oxy radicals in the OH- and Cl-initiated oxidation of ethene, J. Phys. Chem. A, 102, 8116–8123, doi:10.1021/jp981937d, 1998. 1275
Orlando, J. J., Tyndall, G. S., and Paulson, S. E.: Mechanism of the OH-initiated oxidation of methacrolein, Geophys. Res. Lett., 26, 2191–2194, doi:10.1029/1999gl900453, 1999. 1278, 1279
Orlando, J. J., Iraci, L. T., and Tyndall, G. S.: Chemistry of the cyclopentoxy and cyclohexoxy radicals at subambient temperatures, J. Phys. Chem. A, 104, 5072–5079, doi:10.1021/jp0002648, 2000. 1275
Orlando, J. J., Tyndall, G. S., and Wallington, T. J.: The atmospheric chemistry of alkoxy radicals, Chem. Rev., 103, 4657–4689, doi:10.1021/cr020527p, 2003. 1274, 1276
Peeters, J. and Muller, J.-F.: HO_x radical regeneration in isoprene oxidation via peroxy radical isomerisations, II: experimental evidence and global impact, Phys. Chem. Chem. Phys., 12, 14227–14235, doi:10.1039/C0CP00811G, 2010. 1278
Peeters, J., Nguyen, T. L., and Vereecken, L.: HO_x radical regeneration in the oxidation of isoprene, Phys. Chem. Chem. Phys., 11, 5935–5939, doi:10.1039/b908511d, 2009. 1276, 1277
Platt, U., Alicke, B., Dubois, R., Geyer, A., Hofzumahaus, A., Holland, F., Martinez, M., and Stutz, J.: Free radicals and fast photochemistry during BERLIOZ, J. Atmos. Chem., 42, 359–394, 2002. 1259
Qi, B., Takami, A., and Hatakeyama, S.: A calibration method for measurement of small alkyl organic peroxy radicals by chemical amplifier, Anal. Sci., 22, 1091–1093, 2006. 1265
Ren, X., Edwards, G. D., Cantrell, C. A., Lesher, R. L., Metcalf, A. R., Shirley, T., and Brune, W. H.: Intercomparison of peroxy radical measurements at a rural site using laser-induced fluorescence and peroxy radical chemical ionization mass spectrometer (PerCIMS) techniques, J. Geophys. Res., 108, 4605, doi:10.1029/2003JD003644, 2003. 1259

AMTD
4, 1255–1302, 2011

Ren, X., Harder, H., Martinez, M., Falona, I. C., Tan, D., Lesher, R. L., Carlo, P. D., Simpas, J. B., and Brune, W. H.: Interference testing for atmospheric HO_x measurements by laser-induced fluorescence, J. Atmos. Chem., 47, 169–190, 2004. 1259, 1275

Ren, X., Olson, J. R., Crawford, J. H., Brune, W. H., Mao, J., Long, R. B., Chen, Z., Chen, G., Avery, M. A., Sachse, G. W., Barrick, J. D., Diskin, G. S., Huey, L. G., Fried, A., Cohen, R. C., Heikes, B., Wennberg, P. O., Singh, H. B., Blake, D. R., and Shetter, R. E.: HO_x chemistry during INTEX-A 2004: observation, model calculation, and comparison with previous studies, J. Geophys. Res., 113, D05310, doi:10.1029/2007JD009166, 2008. 1259

Sadanaga, Y., Yoshino, A., Watanaba, K., Yoshioka, A., Wakazono, Y., Kanaya, Y., and Kajii, Y.: Development of a measurement system of peroxy radicals using a chemical amplification/laser-induced fluorescence technique, Rev. Sci. Instrum., 75, 864–872, doi:10.1063/1.1666985, 2004. 1257

Saunders, S. M., Jenkin, M. E., Derwent, R. G., and Pilling, M. J.: Protocol for the development of the Master Chemical Mechanism, MCM v3 (Part A): tropospheric degradation of non-aromatic volatile organic compounds, Atmos. Chem. Phys., 3, 161–180, doi:10.5194/acp-3-161-2003, 2003. 1272

Schultz, M., Heitlinger, M., Mihelcic, D., and Volz-Thomas, A.: Calibration source for peroxy radicals with built-in actinometry using H_2O and O_2 photolysis at 185 nm, J. Geophys. Res., 100, 18811–18816, 1995. 1262

Stevens, P. S., Mather, J. H., and Brune, W. H.: Measurement of tropospheric OH and HO_2 by laser-induced fluorescence at low pressure, J. Geophys. Res., 99, 3543–3557, 1994. 1259

Tuazon, E. C. and Atkinson, R.: A product study of the gas-phase reaction of methyl vinyl ketone with the OH radical in the presence of NO_x, Int. J. Chem. Kinet., 21, 1141–1152, doi:10.1002/kin.550211207, 1989. 1278

Tuazon, E. C. and Atkinson, R.: A product study of the gas-phase reaction of methacrolein with the OH radical in the presence of NO_x, Int. J. Chem. Kinet., 22, 591–602, doi:10.1002/kin.550220604, 1990. 1278, 1279

Vereecken, L., Peeters, J., Orlando, J. J., Tyndall, G. S., and Ferronato, C.: Decomposition of β-hydroxypropoxy radicals in the OH-initiated oxidation of propene. A theoretical and experimental study, J. Phys. Chem. A, 103, 4693–4702, doi:10.1021/jp990046i, 1999. 1275

Volkamer, R., Klotz, B., Barnes, I., Imamura, T., Wirtz, K., Washida, N., Becker, K. H., and Platt, U.: OH-initiated oxidation of benzene Part I, Phenol formation under atmospheric conditions, Phys. Chem. Chem. Phys., 4, 1598–1610, doi:10.1039/b108747a, 2002. 1279

AMTD
4, 1255–1302, 2011

Washida, N., Mori, Y., and Tanaka, I.: Quantum yield of ozone formation from photolysis of the oxygen molecule at 1849 and 1931 A, J. Chem. Phys., 54, 1119–1122, doi:10.1063/1.1674946, 1971. 1263

Weber, M.: Entwicklung und Einsatz eines Instrumentes zur Bestimmung der Konzentration von HO_2-Radikalen in der Troposphäre, Ph.D. thesis, Universitaet Koeln, Koeln, 1998. 1259, 1272, 1275

Zhang, D. H., Collins, M. A., and Lee, S.-Y.: First-principle theory for the $H + H_2O$, D_2O reactions, Science, 290, 961–963, 2000. 1264

Zhang, J., Dransfield, T., and Donahue, N. M.: On the mechanism for nitrate formation via the peroxy radical + NO reaction, J. Phys. Chem. A, 108, 9082–9095, doi:10.1021/jp048096x, 2004. 1273

AMTD
4, 1255–1302, 2011

Table 1. Properties of the instrument regarding the HO_2 detection.

	Config. 1	Config. 2[a]
Inlet orifice/mm	0.2	0.4
Sample flow rate/slpm	0.28	1.1
[NO]/10^{12} cm^{-3}	1–40	5–100
Distance nozzle – detection/cm	10	
Distance NO addition – detection/cm	5.5	
Conversion reaction time/ms	0.18[b]	2.7[b]
Cell pressure/hPa	3.5	
Laser rep. rate/kHz	8.5	
Laser power/mW	35–40	
Laser beam diameter/mm	8	
1σ accuracy of the calibration/%	±10	

[a] Configuration during previous field campaigns.
[b] Determined from experiments here.

AMTD
4, 1255–1302, 2011

Table 2. Measured and calculated relative detection sensitivities of different RO_2 species in the HO_2 detection cell for two inlet configurations. Modeled values are calculated from the ratio of conversion efficiencies that are achieved for RO_2 and HO_2 ($\alpha'_{RO_2} = \frac{\epsilon_{RO_2}}{\epsilon_{HO_2}}$) assuming $\gamma_{RO_2} = \gamma_{HO_2}$ (Eq. 11). The sensitivity applies for RO_2 that is produced in the reaction of organic precursors with OH and O_2.

	Orifice 0.4 mm $[NO] = 1.3 \times 10^{14}$ cm^{-3}		Orifice 0.2 mm $[NO] = 1.2 \times 10^{14}$ cm^{-3}	
Precursor	α_{RO_2} (exp.)	α'_{RO_2} (model)	α_{RO_2} (exp.)	α'_{RO_2} (model)
Methane	0.04 ± 0.04	0.04	−0.01 ± 0.02	0.00
Ethane	0.07 ± 0.03	0.18	0.01 ± 0.02	0.00
Cyclohexane	0.48 ± 0.14	0.14[a]	0.03 ± 0.00	0.00[a]
Ethene	0.85 ± 0.05	0.85	0.17 ± 0.03	0.08
Propene	0.95 ± 0.03	0.83	0.15 ± 0.03	0.08
Isoprene	0.79 ± 0.05	0.67	0.12 ± 0.02	0.07
MVK	0.60 ± 0.06	0.26[b]	0.24 ± 0.11	0.03[b]
MACR	0.58 ± 0.04	0.38	0.14 ± 0.02	0.00
Benzene	0.86 ± 0.11[c]	0.78	0.17 ± 0.17[c]	0.08

[a] MCMv3.1 does not include decomposition of the cyclohexoxy radical.
[b] MCMv3.1 does not include all reaction paths of the RO_2 radical from MVK.
[c] Value does not include 65% prompt HO_2 formation in the radical source.

AMTD
4, 1255–1302, 2011

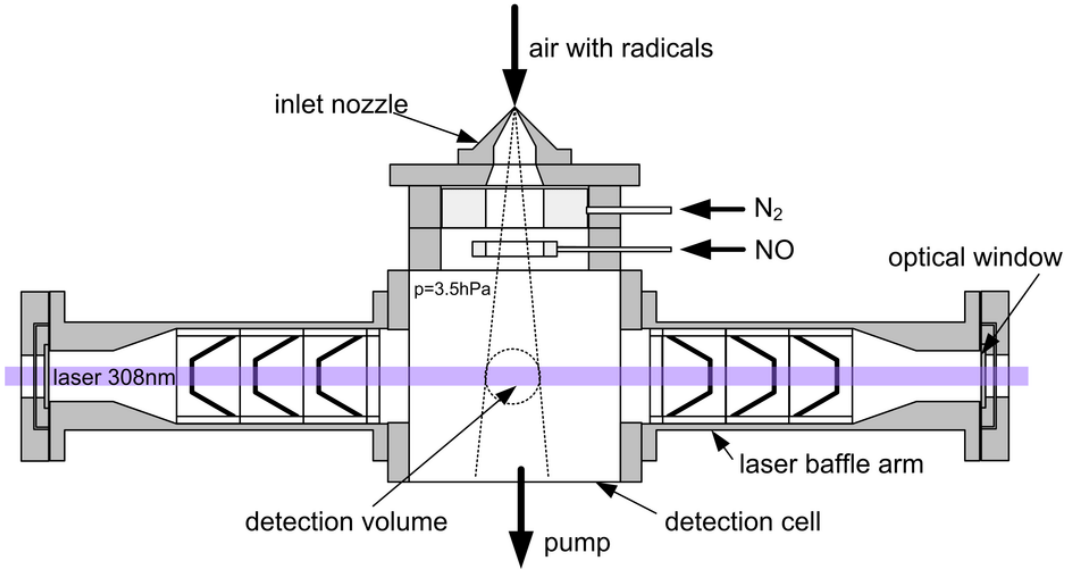

Fig. 1. Schematic drawing of the experimental setup. Peroxy radicals are converted to OH in their reaction with NO, which is injected into the gas expansion downstream of the inlet nozzle, in the low pressure detection cell. The air is exposed to pulsed laser radiation at 308 nm and the resulting fluorescence from OH is detected in the direction perpendicular to the laser and gas beam. For experiments done here, air is sampled from a calibration source, which provides either OH and HO_2, exclusive HO_2 or HO_2 and RO_2 radicals.

AMTD
4, 1255–1302, 2011

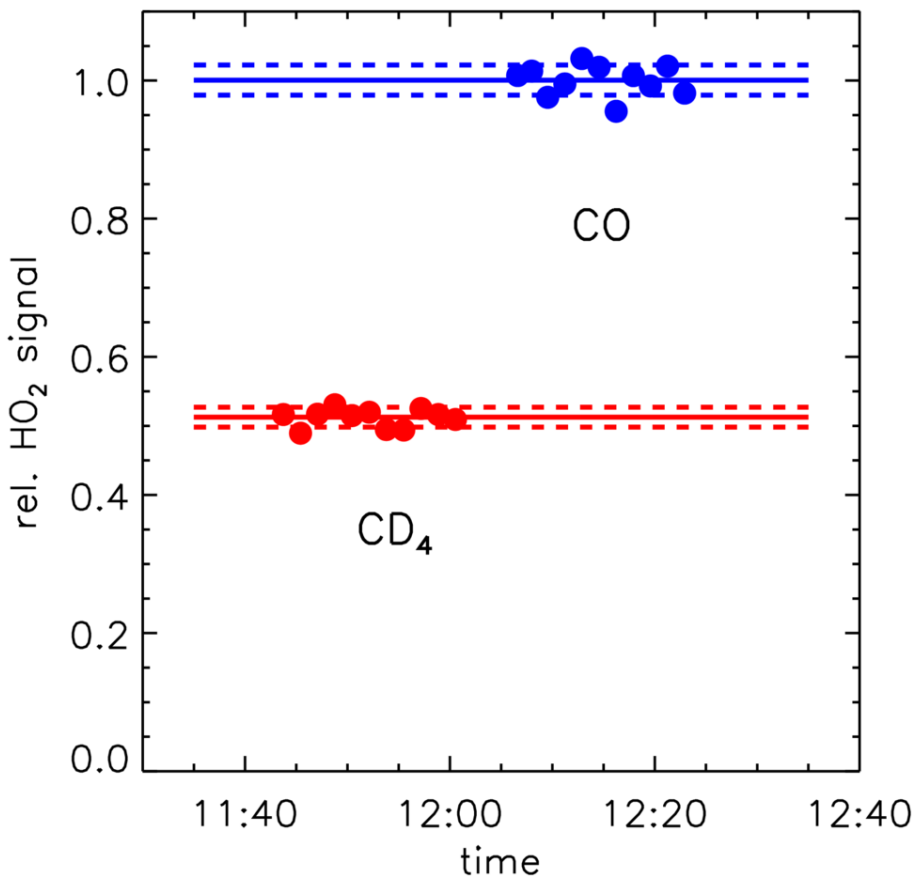

Fig. 2. Relative HO_2 signals if either CO or CD_4 is used as an OH scavenger in the calibration source. Symbols show individual measurement points, solid lines denote average values and dashed lines represent 1σ standard deviations of measurements.

AMTD
4, 1255–1302, 2011

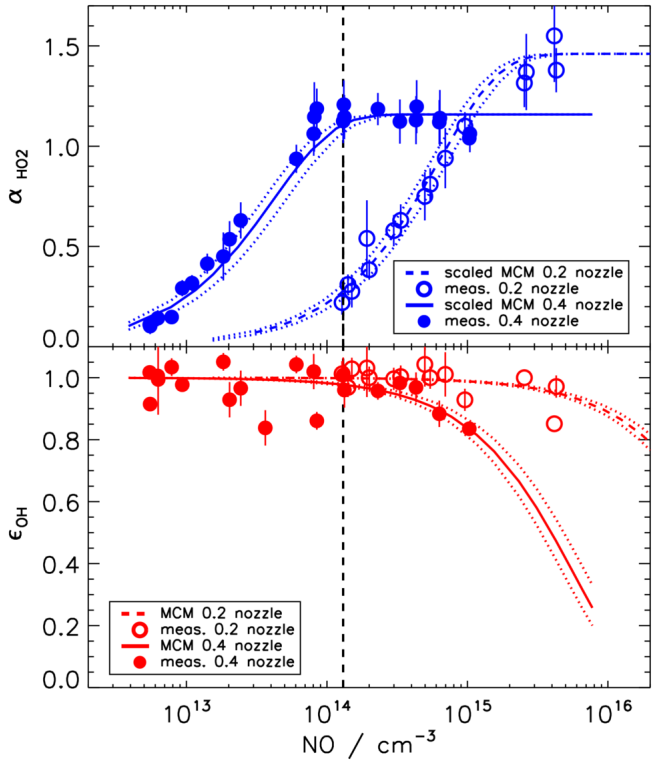

Fig. 3. Relative OH sensitivity (lower panel) and HO_2 (upper panel) conversion efficiency to OH depending on the NO concentration in the detection cell. Measurements (symbols) are compared to calculations using MCMv3.1 (lines). Two inlet nozzles with different orifices (0.2 and 0.4 mm) were used, in order to vary the reaction time for the conversion in the cell (0.18 and 2.7 ms). Dotted lines give results from sensitivity runs of the model varying the reaction time by ±0.025 and ±0.5 ms, respectively. The vertical dashed line indicates the working point for the instrument with the 0.4 mm nozzle in the past.

AMTD
4, 1255–1302, 2011

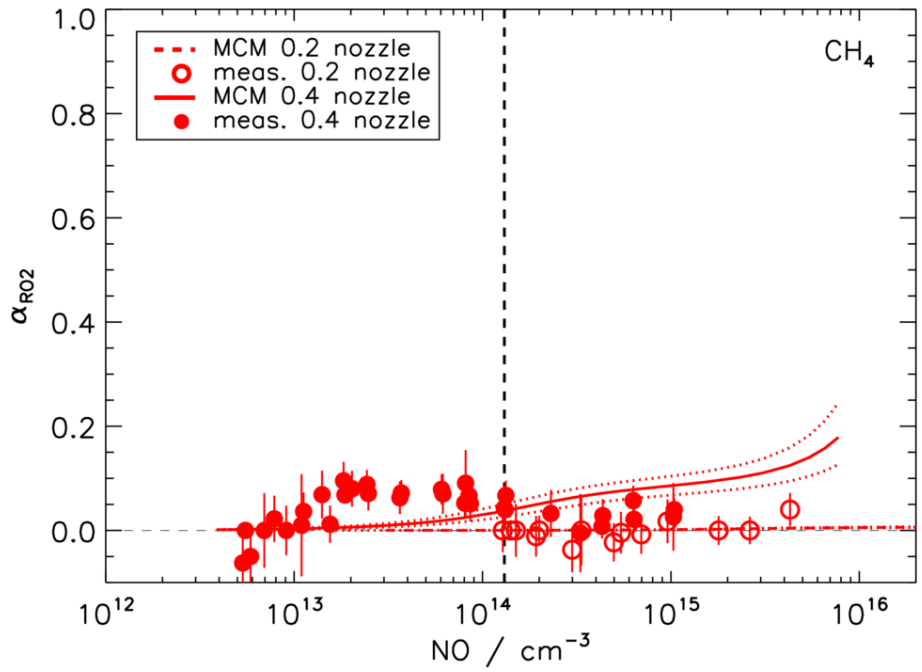

Fig. 4. Relative detection sensitivity for RO_2 radicals produced by methane and OH depending on the NO concentration in the detection cell. Measurements (symbols) are compared to calculations using MCMv3.1 (solid line) with non-zero initial RO_2 and zero HO_2 concentration. Two inlet nozzles with different orifices (0.2 and 0.4 mm) were used, in order to vary the reaction time for the conversion in the cell. Reaction times determined from the HO_2 conversion efficiency were used for model calculations and were varied according to the uncertainty of the reaction time, ±0.025 and ±0.5 ms (dotted lines). The vertical dashed line indicates the working point for the instrument with 0.4 mm nozzle in the past.

AMTD
4, 1255–1302, 2011

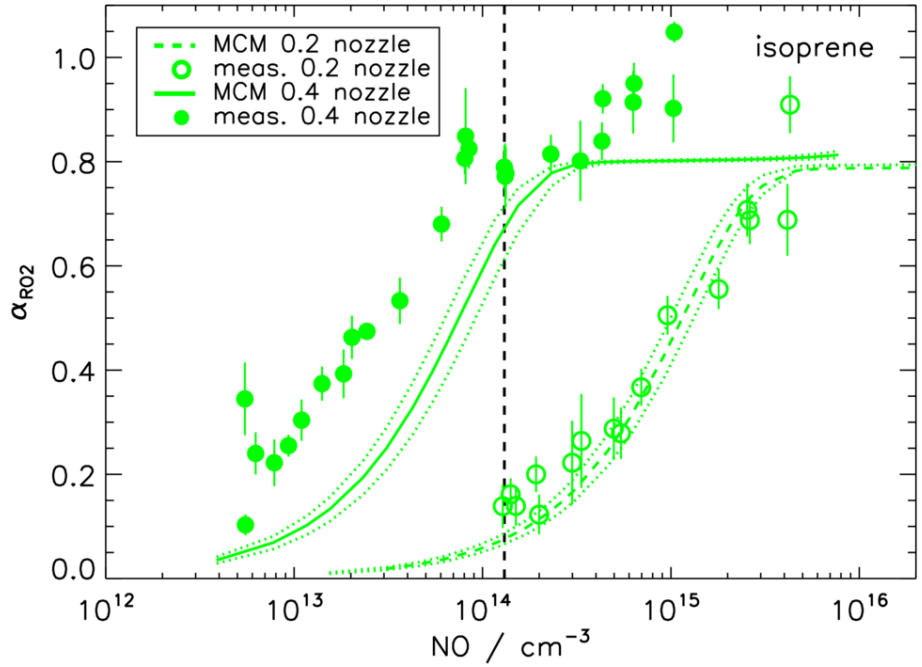

Fig. 5. Same as Fig. 4, but for RO_2 radicals produced by isoprene and OH.

AMTD
4, 1255–1302, 2011

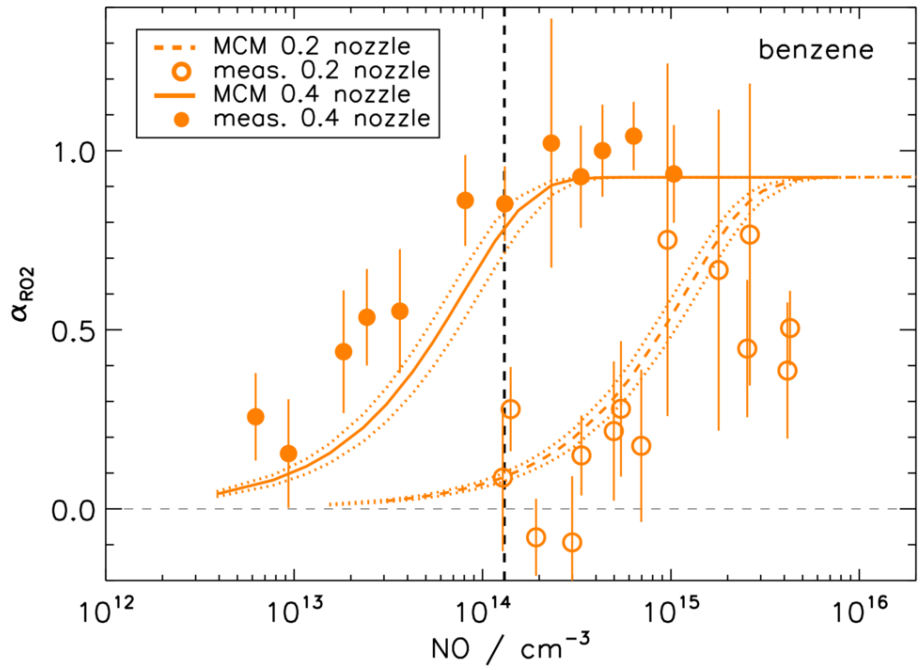

Fig. 6. Same as Fig. 4, but for RO_2 radicals produced by benzene and OH. Measurements take 65% of prompt HO_2 formation in the radical source into account.

AMTD
4, 1255–1302, 2011

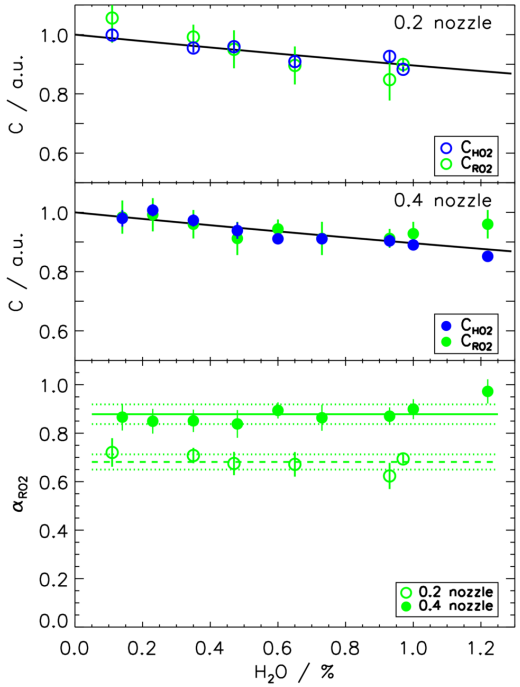

Fig. 7. Dependence of the interference from RO_2 radicals produced by isoprene and OH on water vapor (lower panel) at high NO concentrations (0.2 mm nozzle: 3×10^{15} cm^{-3}, 0.4 mm nozzle: 4×10^{14} cm^{-3}). Experiments were carried out for two combinations of reaction times (orifice diameters) and NO concentrations. Symbols show individual measurement points and lines are average values (solid, dashed) and 1σ standard deviations (dotted) of measurements. In the upper two panels the water vapor dependence of measured detection sensitivities for HO_2, C_{HO_2}, and RO_2 from isoprene, C_{RO_2}, (scaled to one dry conditions) is compared to calculations that give the reduction of the instrument sensitivity due to fluorescence quenching by water vapor (black lines).

AMTD
4, 1255–1302, 2011

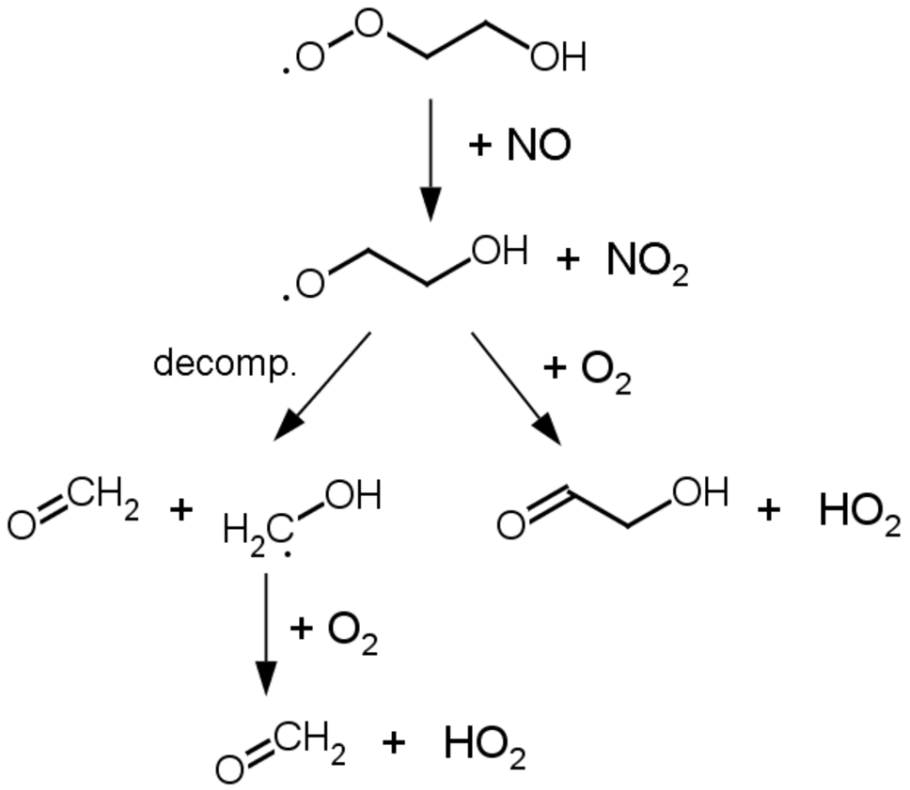

Fig. 8. Reaction scheme of the radical sequence of the β-hydroxyalkyl peroxy radical produced by the reaction of OH with ethene. The β-hydroxyalkoxy radical formed in the reaction with NO either decomposes or reacts with O_2 in contrast to other β-hydroxyalkoxy species which exclusively decompose.

AMTD
4, 1255–1302, 2011